Calcium-dependent inactivation of calcium channels in cochlear hair cells of the chicken

Seunghwan Lee[2], Olga Briklin[1], Hakim Hiel[1] and Paul Fuchs[1]

[1]*Center for Hearing and Balance, Department of Otolaryngology, Head and Neck Surgery, and Center for Sensory Biology, Johns Hopkins University School of Medicine, Baltimore, MD 21205, USA*
[2]*Department of Otolaryngology – Head & Neck Surgery, Hanyang University, Seoul, Korea*

Voltage-gated calcium channels support both spontaneous and sound-evoked neurotransmitter release from ribbon synapses of cochlear hair cells. A variety of regulatory mechanisms must cooperate to ensure the appropriate level of activity in the restricted pool of synaptic calcium channels (∼100) available to each synaptic ribbon. One potential feedback mechanism, calcium-dependent inactivation (CDI) of voltage-gated, L-type calcium channels, can be modulated by calmodulin-like calcium-binding proteins. CDI of voltage-gated calcium current was studied in hair cells of the chicken's basilar papilla (analogous to the mammalian cochlea) after blocking the predominant potassium conductances. For inactivating currents produced by 2.5 s steps to the peak of the current–voltage relation (1 mM EGTA internal calcium buffer), single exponential fits yielded an average decay time constant of 1.92 ± 0.18 s (mean ± S.E.M., $n = 12$) at 20–22°C, while recovery occurred with a half-time of ∼10 s. Inactivation produced no change in reversal potential, arguing that the observed relaxation did not result from alternative processes such as calcium accumulation or activation of residual potassium currents. Substitution of external calcium with barium greatly reduced inactivation, while inhibition of endoplasmic calcium pumps with t-benzohydroquinone (BHQ) or thapsigargin made inactivation occur faster and to a greater extent. Raising external calcium 10-fold (from 2 to 20 mM) increased peak current 3-fold, but did not alter the extent or time course of CDI. However, increasing levels of internal calcium buffer consistently reduced the rate and extent of inactivation. With 1 mM EGTA buffering and in 2 mM external calcium, the available pool of calcium channels was half-inactivated near the resting membrane potential (−50 mV). CDI may be further regulated by calmodulin-like calcium-binding proteins (CaBPs). mRNAs for several CaBPs are expressed in chicken cochlear tissue, and antibodies to CaBP4 label hair cells, but not supporting cells, equivalent to the pattern seen in mammalian cochlea. Thus, molecular mechanisms that underlie CDI appeared to be conserved across vertebrate species, may provide a means to adjust calcium channel open probability, and could serve to maintain the set-point for spontaneous release from the ribbon synapse.

(Resubmitted 1 May 2007; accepted after revision 24 July 2007; first published online 26 July 2007)
Corresponding author P. Fuchs: The Johns Hopkins University School of Medicine, 818 Ross Building, 720 Rutland Avenue, Baltimore, MD 21205, USA. Email: pfuchs@jhmi.edu

Voltage-gated calcium channels (VGCCs) in hair cells provide the trigger for both spontaneous and sound-evoked activity of cochlear afferent neurons (Robertson & Paki, 2002). In amphibia (Lewis & Hudspeth, 1983; Roberts *et al.* 1990; Prigioni *et al.* 1992; Rodriguez-Contreras & Yamoah, 2001), reptiles (Art & Fettiplace, 1987; Art *et al.* 1993; Schnee & Ricci, 2003), birds (Fuchs *et al.* 1990; Zidanic & Fuchs, 1995) and mammals (Nakagawa *et al.* 1991; Beutner & Moser, 2001; Engel *et al.* 2002; Bao *et al.* 2003; Marcotti *et al.* 2003; Michna *et al.* 2003), evidence consistently shows that the majority of hair cell calcium channels are 'L-type'. That is, they are dihydropyridine sensitive, and preferentially permeant to barium over calcium. Some studies, particularly in vestibular hair cells, have identified a distinctive minority of channels that are dihydropyridine *in*sensitive (Su *et al.* 1995; Rodriguez-Contreras & Yamoah, 2001). The L-type calcium channel of hair cells is encoded by the α1D or $Ca_V1.3$ gene (Green *et al.* 1996; Kollmar *et al.* 1997*b*; Platzer *et al.* 2000; Ramakrishnan *et al.* 2002; Brandt *et al.* 2003; Michna *et al.* 2003; Dou *et al.* 2004; Hafidi & Dulon, 2004). VGCCs in most hair cells activate and deactivate

 DOI: 10.1113/jphysiol.2007.135582

rapidly (within less than 1 ms) and remain open during 100–200 ms commands to membrane potentials positive to −40 mV, showing little or no inactivation. This has long been viewed as consistent with the role of these channels in spontaneous, as well as sound-evoked, transmitter release from hair cells. More recently however, evidence has been found for slow, seconds-long inactivation of voltage-gated calcium currents in hair cells of amphibia (Rispoli *et al.* 2000; Martini *et al.* 2004), reptiles (Schnee & Ricci, 2003), and the inner (Marcotti *et al.* 2003) and outer (Michna *et al.* 2003) hair cells of the mammalian cochlea. Does this inactivation have functional relevance and if so, how is it reconciled with the requirement for steady-state gating? The implication is that additional processes must exist to modulate inactivation. That is, such modulation would serve to ensure spontaneous activity, and at the same time, an adequate dynamic range for sound-evoked gating of the limited number of calcium channels (∼100) thought to operate at each ribbon synapse (Roberts *et al.* 1990; Martinez-Dunst *et al.* 1997; Brandt *et al.* 2005; Fuchs, 2005), emphasized by the fact that each ribbon is the sole input for a single auditory neuron in mammals. Also, such a mechanism could contribute to differences in spontaneous rate among cochlear afferent neurons (Merchan-Perez & Liberman, 1996).

Calcium-dependent inactivation (CDI) of L-type calcium channels is mediated by calmodulin (Liang *et al.* 2003), raising the possibility that the extent of CDI could be regulated by calmodulin-like calcium-binding proteins (CaBPs). Indeed, recent work has shown that calmodulin-dependent CDI of $Ca_V1.3$ is diminished by heterologous coexpression with CaPBs (Yang *et al.* 2006). One of these, CaBP4, is preferentially expressed in retinal photoreceptors (Haeseleer *et al.* 2004) and cochlear inner hair cells (Yang *et al.* 2006), both employing ribbon synapses. Still further heterogeneity of CDI may result from alternative splicing of the $Ca_V1.3$ α subunit to eliminate portions of the calmodulin-binding 'IQ' domain (Shen *et al.* 2006).

The present work seeks to characterize CDI and to nominate potential molecular mechanisms in chicken auditory hair cells. The chicken basilar papilla ('cochlea') is a tonotopically organized sensory epithelium (Chen *et al.* 1994) containing some 10,000 hair cells differentially innervated by afferent and efferent nerve fibres (Fischer, 1992). Avian (chicken) hair cells share features in common with those of cold-blooded vertebrates, as well as with those of mammals. Spontaneous afferent activity has preferred intervals (Salvi *et al.* 1992), presumably reflecting the electrical resonance in chicken auditory hair cells (Fuchs *et al.* 1988) like that shown previously in turtles (Crawford & Fettiplace, 1981). As in mammals, a subset of hair cells of chickens, 'tall hair cells', are preferentially innervated by afferent nerve fibres, possess numerous presynaptic structures (ribbons) and have relatively large voltage-gated calcium currents (Martinez-Dunst *et al.* 1997). Corresponding tonotopic gradients occur in the expression of calcium-buffering proteins such as calbindin (Hiel *et al.* 2002). Finally, developmental changes in ion channel expression by chicken hair cells (Fuchs & Sokolowski, 1990) parallel those observed in the mammalian cochlea (Kros *et al.* 1998). The chicken otocyst and basilar papilla provide a useful model system for *in vitro* developmental studies (Sokolowski *et al.* 1993), and an important source of comparative information. We have examined the slow inactivation of calcium currents in tall hair cells of the chicken's basilar papilla, analogous to inner hair cells of the mammalian cochlea. The expectation is that basic molecular mechanisms of calcium channel modulation that are conserved throughout vertebrates should be evident here.

Methods

The basilar papilla (auditory sensory epithelium) was dissected from the temporal bone of chickens (*Gallus gallus*, 1–21 days old), after they had been deeply anaesthetized (intramuscular pentobarbitol) and decapitated, according to a protocol (no. AV04M160) approved by the Institutional Animal Care and Use Committee of Johns Hopkins University. Procedures for inner ear microdissection and isolation of hair cells essentially followed those published previously (Fuchs *et al.* 1988). The excised basilar papilla (auditory epithelium) was treated briefly with protease (0.1 mg ml^{-1} protease type XXIV, Sigma-Aldrich) to facilitate the removal of the overlying tectorial membrane. 'Tall' hair cells (analogous to inner hair cells in the mammalian cochlea) were aspirated from a region 1.0–1.2 mm from the apical tip of the papilla, and then dispersed into a recording chamber.

Whole-cell, gigohm-seal voltage clamp

Whole-cell, patch-clamp recordings were made from the isolated hair cells as previously described (Fuchs & Evans, 1990; Fuchs *et al.* 1990) using commercially available equipment and software (Axon Instruments 200B, pCLAMP). Patch pipettes (5–10 MΩ resistance) were coated with Sylgard or ski wax to reduce capacitance. The seal resistance before breaking into the whole-cell recording mode was always > 2 GΩ. In the standard 'inactivation protocol', the membrane was clamped to the potential at which calcium current was maximal (between −20 and 0 mV) for 2 s. The extent of inactivation was determined as the fractional drop in current amplitude during that step. For example, a reduction from 100 pA to 30 pA would constitute 70% inactivation. The time constant of inactivation was taken from a single

exponential fit to the entire 2 s-long inward current. The cell was allowed to recover for 60 s between successive inactivation protocols. In other experiments a 100 mV, 100 ms-long voltage ramp was used to assess calcium current magnitude, voltage dependence and reversal potential before and following an inactivating voltage step. The same voltage ramp was also used to assess the calcium current *I–V* relation from different holding potentials, ranging from ∼ −90 to −50 mV. In these latter experiments the extent of inactivation was taken as the ratio of peak currents obtained during *I–V* ramps from different holding potentials.

Both internal and external saline solutions were designed to block predominant potassium currents that normally overlie and obscure the smaller voltage-gated calcium currents of hair cells. The internal (pipette) solution contained (mM): 140 $CsMeSO_4$, 10 Hepes, 3 Mg_2ATP, 5 phosphocreatine, 5.6 glucose, and pH to 7.3; 290 mosmol l^{-1}. This was modified to provide a range of calcium buffer concentrations as noted in Results. The standard external saline contained (mM): 90 NaCl, 6 KCl, 1 $MgCl_2$, 10 Hepes, 30 tetraethyl-ammonium chloride (TEA), 5.6 glucose, 2 pyruvate, 3,4-aminopyridine, and 500 nM apamin, pH 7.3, 310 mosmol l^{-1}. The measured junction potential was ∼ −10 mV and this has been added to the reported values. Divalent cations (calcium or barium) were added as 2 or 20 mM of the chloride salt. Compounds designed to alter calcium-dependent inactivation were dissolved into external saline and perfused into the bath after initial recordings in control conditions. All tissue preparation, cell isolation and recordings were conducted at room temperature (20–22°C).

Reverse-transcriptase polymerase chain reaction from chicken basilar papilla

Basilar papillae were quickly removed from the severed head and stored on dry ice. RNA was extracted with TRIzol reagent, chloroform, isopropyl alcohol and RNase free water, and subjected to reverse transcription with oligo(dT)12–18 primers. Polymerase chain reactions (30 cycles) were run with primers specific for each of the three chicken CaBP orthologues identified from a homology search of the chicken genome (NCBI http://www.ncbi.nlm.nih.gov/genome/guide/chicken/). Amplified cDNAs were separated on gels, and bands of the predicted size cut out, subcloned into bacteria, excised, purified and sequenced (Johns Hopkins Sequencing Center).

Immunohistology

The inner ear was fixed *in situ* for 1 h by perfusion with 2% paraformaldehyde. The otic capsule was dissected free and immersed in fixative for 2–3 h more. The entire capsule was then prepared for cryosectioning at 10–14 μm thickness. Mounted sections were exposed to goat anti-ChAT (Chemicon) and rabbit anti-CaBP4, or rabbit anti-CaBP1 (both CaBP antibodies from F. Haeseleer, University of Washington, Seattle, WA). Secondary antibodies were conjugated to Alexa 488 or Alexa 555. Labelled sections were viewed and photographed on an upright Nikon fluorescence microscope.

Results

Potassium blockers isolate hair cell calcium current

Hair cells were isolated from a region approximately 1 mm from the apical tip of the basilar papilla, corresponding to approximately 1 kHz along the tonotopic axis (Chen *et al.* 1994). As in mammals, auditory hair cells in birds can be subdivided based on the pattern of innervation and cross-cochlear position. 'Tall' hair cells in chickens are analogous to inner hair cells of mammals, having the majority of afferent synaptic contacts and little if any efferent innervation (Fischer, 1992). In contrast, chicken short hair cells have efferent, rather than afferent innervation (Zidanic, 2002). Consistent with this differential synaptic function, tall hair cells consistently have larger voltage-gated calcium currents than do short hair cells (Martinez-Dunst *et al.* 1997).

The membrane conductance of chicken hair cells is dominated by voltage-gated potassium channels (Fig. 1*A*, 5 mM external calcium, holding voltage −64 mV). Thus, recording conditions were designed to eliminate the predominant potassium currents and reveal the smaller, usually covert, voltage-gated calcium currents. This involved a panel of potassium channel blockers, and elevating external calcium to enlarge usually small currents through these channels (Fuchs *et al.* 1990; Martinez-Dunst *et al.* 1997). The standard protocol used 20 mM external calcium, and holding voltages of −70 mV (Fig. 1*B*, *C* and *D*), negative to the activation range of the calcium channels (Zidanic & Fuchs, 1996). Internal caesium completely eliminated the rapidly activating calcium-sensitive (BK) potassium current of these hair cells. However, especially in the 'tallest' hair cells, whole-cell recordings still showed substantial outward currents at positive membrane potentials, as well as large, slow inward tail currents (Fig. 1*B*). These residual currents probably result from the significant numbers of slowly gating delayed rectifier and inward rectifier channels found in this cell type (Murrow, 1994). These voltage-gated currents are particularly problematic because they are blocked by the external barium that was used for differentiating calcium-dependent inactivation of inward currents. Thus, 30 mM TEA and 3 mM 4-aminopyridine (4-AP) were added to the external saline. This combination eliminated slow tail currents and effectively isolated inward

calcium currents (Fig. 1*C*). The peak leak-corrected membrane current was inward up to +60 mV on average (+59.5 ± 1.0 mV, mean ± S.E.M., $n = 28$), and did not vary as a function of calcium buffer (see later).

Under these conditions, prolonged depolarizing voltage steps then produced inward currents that decayed gradually (Fig. 1*D*). The mean time constant of decay obtained for maximal inward currents was 1.92 ± 0.17 s, ± S.E.M., $n = 12$) at room temperature. This slow inactivation is the focus of this work and subsequent experiments will demonstrate that it results largely from calcium-dependent inactivation (CDI) of the hair cell's L-type calcium channels. Before doing so, however, one further control experiment was required: a test for possible contributions from calcium-dependent potassium currents through small-conductance (SK) channels (Matthews *et al.* 2004). These are ordinarily activated through the release of acetylcholine at the efferent synapses (Yuhas & Fuchs, 1999) that are found on short hair cells. If also present in these tall hair cells, SK channels could be activated during prolonged voltage-gated calcium influx, as has been shown in reptilian (Tucker & Fettiplace, 1996) and mammalian hair cells (Marcotti *et al.* 2004) and their contribution might then be mistaken for calcium-dependent inactivation of calcium current. However, exposure to the SK channel blocker apamin at concentrations 10 times those that block hair cell channels (Yuhas & Fuchs, 1999) produced no change in decay of the inward current (or amplitude of the subsequent tail current) produced by a long depolarization (Fig. 1*D*), suggesting that few if any SK channels are available in these tall hair cells. Nevertheless, 500 nM apamin was added to the external saline throughout these studies to assure that all SK activity was eliminated.

Parameters of inactivation

As an additional assessment of the ionic basis of slow inactivation, the voltage dependence and reversal potential of calcium current was measured with a 100 mV, 100 ms-long voltage ramp just before, and immediately after a 2 s inactivating step. If 'inactivation' results from calcium accumulation or contamination by residual

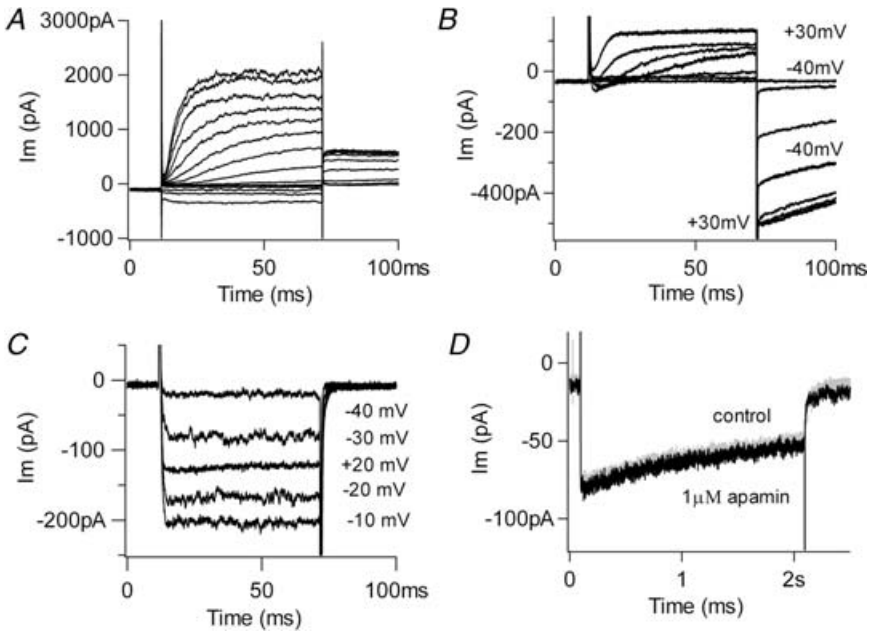

Figure 1. Isolation of calcium current
A, selected membrane currents produced by 60 ms-long voltage commands (−100 to +30 in 10 mV steps) in a chicken cochlear hair cell (holding potential −64 mV). The external solution contained 5.6 mM calcium and the internal saline was buffered with 10 mM EGTA. No potassium channel blockers were used. The observed currents include those through large-conductance (BK) potassium channels, delayed rectifier and inward rectifier K^+ channels (inward currents produced during negative voltage steps). *B*, selected membrane currents produced by indicated voltage commands with internal caesium and 20 mM external calcium (holding voltage −70 mV). Residual unblocked delayed rectifier channels carry the outward currents positive to −40 mV, and inward rectifier channels may contribute to the slow tail currents. *C*, hair cell membrane currents produced by indicated voltage commands as in *B*, but with addition of external TEA and 4-AP. Purely inward currents are visible up to +20 mV and no slow tail currents are seen. *D*, inward currents produced by a 2 s step to 0 mV with TEA and 4-AP in the external saline (holding voltage −70 mV). Addition of 1 μM apamin caused no additional change, arguing that little or no SK current was present. External calcium 20 mM in *C* and *D*.

unblocked potassium channels, rather than a simple closure of calcium channels, the reversal potential should undergo a negative shift as a function of 'inactivation'. In particular, SK channels in chicken hair cells are permeant to Cs^+ as well as K^+ (Yuhas & Fuchs, 1999), yielding a negative equilibrium potential under these recording conditions. Although the calcium current fell by more than 50% in the illustrated cell, the leak-corrected *I–V* relation showed no significant change in shape or in the location of the reversal potential, ∼ +70 mV in this cell (Fig. 2*A*).

Given the seconds-long onset of inactivation, it was necessary also to determine the rate of recovery so that repeated measures could be made on a single cell without risking accumulation of inactivation. The rate of recovery from inactivation was delineated by applying voltage ramps at various times after an inactivating voltage step to a maximally activating voltage (1 mM EGTA internal, 20 mM calcium external). Under these conditions, a test ramp 100 ms after a 2 second-long inactivating step produced a peak inward current that was ∼50% smaller than one immediately before the inactivating step. Over the course of approximately 10 s, the peak inward current recovered nearly completely (Fig. 2*B*). The recovery half-time derived from a single exponential fit was 10.5 s. However, there was considerable variability between cells, and this value ranged from 5.9 to 47.9 s (95% confidence limits). To avoid residual inactivation, standard protocols were spaced at least 60 s apart throughout these experiments.

We also sought to determine whether there was significant intercellular variability in the extent of inactivation. Calcium current magnitude (but not cell volume) varies significantly among chicken auditory hair cells (Martinez-Dunst *et al.* 1997). Thus it was of interest to determine whether inactivation varied as a function of calcium current amplitude among different hair cells, perhaps offering insights into underlying mechanisms. Maximal current amplitude in 20 mM calcium (obtained from the *I–V* relation) was compared to the percentage inactivation (the percentage change in current amplitude during a 2 s inactivating voltage step) among the population of cells buffered with different concentrations of EGTA. However, no correlation was found. Lines fitted through points for each group of cells with a given buffer concentration had slopes not different from zero (Fig. 2*C*). Nor was any correlation found in cells buffered with BAPTA (not shown). This lack of correlation argues that current magnitude, i.e. calcium accumulation *per se*, did not determine the extent of inactivation. In particular, buffer saturation is unlikely to play a significant role, since even with minimal internal buffering (0.1 mM), calcium current size did not predict the extent of inactivation between cells. However, as is evident from the vertical displacement of the fit for each group of cells, the extent of inactivation appeared to vary with the concentration of calcium buffer. This is shown further in Fig. 5.

Calcium current inactivation was measured during 2 s steps to voltages ranging up to +20 mV (Fig. 3*A*).

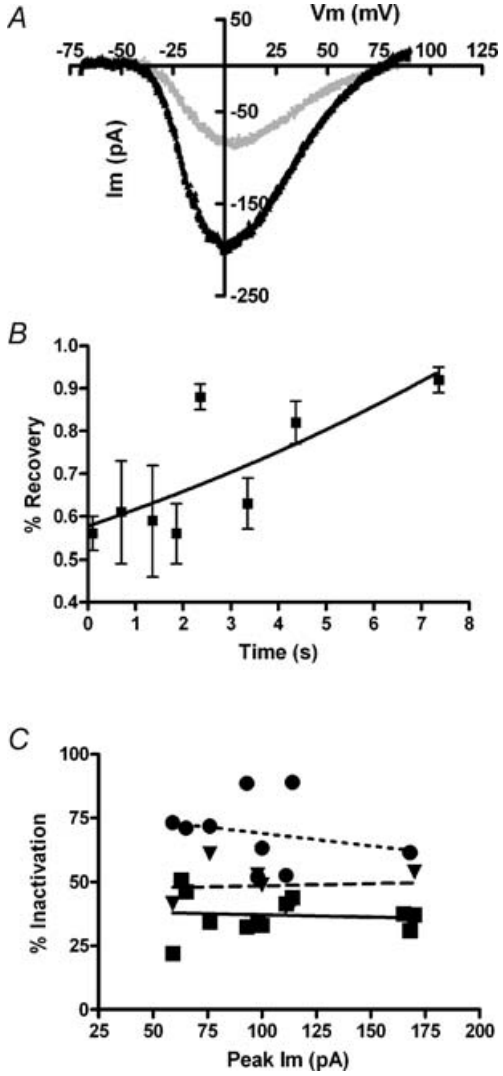

Figure 2. Characterization of inactivation
A, current produced in 20 mM external calcium (1.0 mM EGTA internal buffering) during 100 mV/100 ms voltage ramp 100 ms before, and 100 ms after, a 2 s depolarization to 0 mV that produced 60% inactivation (holding voltage −70 mV). Each *I–V* relation was corrected for the linear leak calculated between −70 and −60 mV. After leak correction the reversal potential was +74 mV before and +82 mV after inactivation. *B*, recovery from inactivation (peak current as percentage of control, from voltage ramps as in *A*, measured at successive times after a 2 s inactivating step to 0 mV (20 mM external calcium, 1.0 mM EGTA internal buffering). Calculated doubling time (single exponential fit) was 10.5 s with r^2 only 0.59; 95% confidence interval from 5.9 to 47.9 s. *C*, percentage inactivation (during 2 s depolarization) as a function of peak calcium current in each cell (20 mM external calcium). Different concentrations of EGTA are indicated by the symbols (● = 0.1 mM, ▼ = 1.0 mM, ■ = 10 mM). Linear fits through each buffer condition have slopes not statistically different from zero. The relation between buffer concentration and percentage inactivation is shown in detail in Fig. 5.

Inactivation, that is the percentage loss of current during the voltage step, was minimal negative to −30 mV and maximal positive to 0 mV (Fig. 3*B*), and in some cases fell again at more positive voltages (Fig. 3*A*) corresponding roughly with the peak of the *I–V* curve for calcium. The mean percentage inactivation for eight cells as a function of membrane potential shows that this behaviour was consistent, essentially saturating positive to 0 mV. Significantly reduced inactivation was not always seen at +20 mV (Fig. 3*B*) and still stronger depolarization usually damaged the cells. This form of voltage dependence also argues against substantial contamination by voltage-activated delayed rectifier-type potassium currents, since these should rise steeply at more positive membrane potentials (Fig. 1*B*).

Calcium dependence of CDI

Substitution of external calcium (20 mM) with barium (20 mM) enlarged the inward currents (Fig. 4*A*). However, inactivation was considerably reduced and slowed with barium as charge carrier (Fig. 4*B*). In the illustrated records (peak currents normalized) inactivation reached 75% in calcium and 15% in barium, while the time constant of inactivation was 1.2 s in calcium and 5.0 s in barium (group averages are given in Fig. 5). In addition to showing a requirement for calcium influx, the identical (essentially zero) slow tail currents in calcium and barium confirmed that little contamination by slow inward rectifier channels remained in these recording conditions (compare to Fig. 1*B*), since inward rectifier channels in chicken hair cells are blocked by external barium (Fuchs *et al.* 1990). Note also that the illustrated cell was weakly buffered with 0.1 mM EGTA, associated with stronger inactivation than seen with 1 or 10 mM EGTA (see Fig. 5).

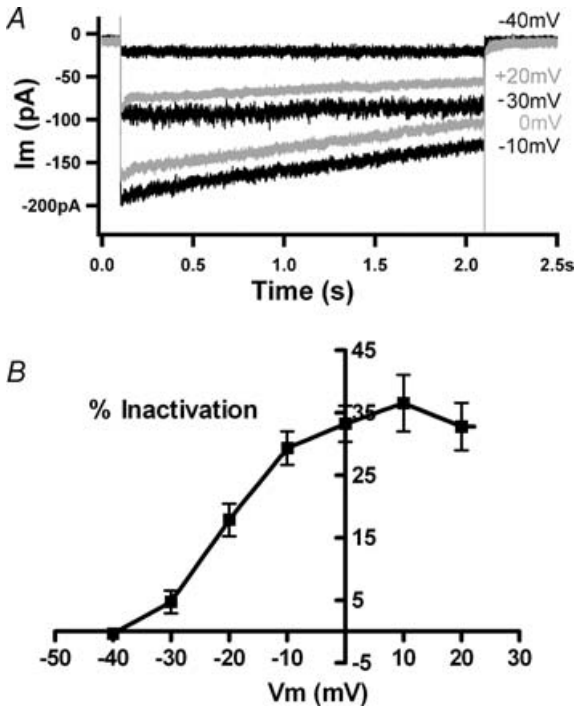

Figure 3. Voltage dependence of calcium-dependent inactivation
A, currents recorded in 20 mM external calcium during a family of 2 s voltage commands to the indicated membrane potentials (holding voltage −70 mV). At −40 and −30 mV little or no inactivation occurred. Maximal inactivation occurred at 0 and +10 mV, while inactivation decreased at +20 mV. Internal calcium buffered with 10 mM BAPTA. *B*, the percentage inactivation in 20 mM calcium at different membrane potentials averaged (± S.E.M.) from 7 cells (4 with 10 mM BAPTA, 2 with 1 mM EGTA, 1 with 0.1 mM EGTA). Inactivation rose as the membrane was depolarized between −40 and 0 mV, then reached a plateau with no significant differences between means at positive membrane potentials (by ANOVA).

Substitution with barium demonstrated a requirement for calcium influx for inactivation to occur. The seconds-long time course further implies that relatively slow mechanisms such as endoplasmic calcium pumping could modulate the underlying cytoplasmic calcium signal. This possibility was examined using compounds that inhibit the activity of endoplasmic calcium (SERCA) pumps (e.g. tert-benzo-hydroquinone (BHQ) and thapsigargin). In cells buffered with 1 mM EGTA, inactivation became faster after treatment with 50 μM BHQ (Fig. 4*C*). During exposure to SERCA blockers the time course of inactivation was better fitted with a double, rather than single exponential, due to the appearance of a faster (τ ∼100 ms) initial rate of decay. The origin of this process was not determined, but it did require that control records also be fitted with double exponentials. Nonetheless, in five cells, the second, slower time constant of decay (over the last 1.8 s) was faster in the presence of BHQ, 1.18 s (± 0.7 s, S.E.M.), than in control conditions for those same cells, 1.71 s (±0.3 s, S.E.M.). Correspondingly, the extent of inactivation was approximately doubled after SERCA block (Fig. 4*D*). Thapsigargin (10 μM) had a nearly equivalent effect, producing a 1.8-fold increase in the extent of inactivation in four cells (Fig. 4*D*). The effects of the SERCA blockers were not reversible during the time course of these recordings.

The effect of cytoplasmic buffering on CDI

To explore further the calcium dependence of inactivation, the standard recording protocols were repeated using internal (pipette) solution containing EGTA or BAPTA at concentrations ranging from 0.1 to 10 mM. In keeping with its hypothesized calcium dependence, the degree of inactivation varied with buffer concentration. Lower concentrations of buffer resulted in faster, more extensive inactivation (Fig. 5*A*). Averaged time constants obtained from each group suggested a progressive slowing with higher buffer concentrations, as well as generally slower

time constants in BAPTA than in EGTA (Fig. 5*B*). However, statistical tests (ANOVA) showed significance ($P < 0.05$) only between the lowest buffer concentration (EGTA or BAPTA) and any other groups with 20 mM external calcium. The loss of significance arose primarily from increased variance in higher buffer conditions, presumably reflecting the difficulty of extrapolating fits beyond the 2 s time course of the conditioning voltage step.

Given the uncertainty of extrapolated time constant measures with strong buffering, it proved useful alternatively to measure the extent of inactivation that also varied systematically with the internal buffer concentration (cf. Fig. 2*C*). Inactivation (the fraction of current lost) reached an average value of $66 \pm 3.1\%$ ($\pm$ S.E.M., $n = 14$) in 0.1 mM EGTA, $48 \pm 2.1\%$ ($n = 14$) in 1 mM EGTA, and $37 \pm 2.2\%$ ($n = 12$) in 10 mM EGTA (Fig. 5*C*). All these means were significantly different ($P < 0.05$ by ANOVA). Inactivation averaged approximately 17% when barium was substituted for calcium and this residual level had no significant correlation with buffer concentration. Although it did not reach statistical significance, the average peak current was largest in the highest buffer concentration (~120 pA in 10 mM EGTA compared to ~100 pA in 0.1 mM EGTA). Finally, there were no significant differences in the reversal potential measured during voltage ramps in the different buffering conditions.

A second series of experiments was undertaken with BAPTA rather than EGTA as the internal calcium buffer. Here a similar relationship was obtained, with stronger inactivation for lower concentrations of buffer, with mean

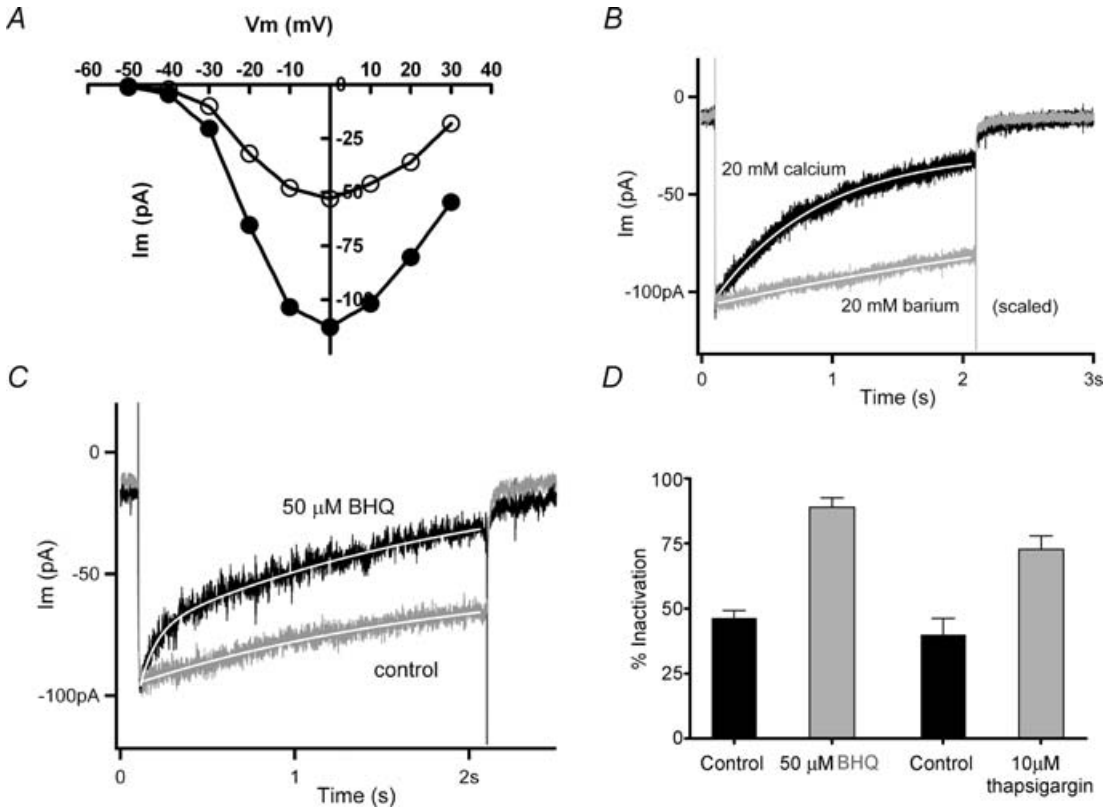

Figure 4. The effects of calcium influx and internal stores
A, current–voltage relation obtained with 20 mM calcium or barium in the external saline (holding voltage −70 mV). Barium current was on average twice the amplitude of calcium current in all cells tested. *B*, a 2 s step to 0 mV from a holding voltage of −70 mV produced a slowly decaying inward current ($\tau = 0.8$ s, from single exponential fit, continuous white line) carried by 20 mM calcium (0.1 mM EGTA buffering). Substitution with barium yielded a larger current (scaled by 0.63) that decayed much more slowly ($\tau = 6.5$ s, from single exponential fit, continuous white line). *C*, membrane current during a 2 s step to 0 mV before ('control') and 4 min after the addition of 50 μM SERCA blocker benzo-hydroquinone ('50 μM BHQ') (20 mM calcium external, 1.0 mM EGTA internal buffer, holding voltage −70 mV). Inactivation was more extensive in the SERCA blocker. Peak control current was scaled by 0.8. Continuous white line indicates double exponential fit to each record. *D*, the percentage inactivation in control ($46.2 \pm 2.9\%$, mean $\pm$ S.E.M., $n = 5$), 50 μM BHQ ($88.9 \pm 3.5\%$, $n = 5$), control ($40 \pm 11\%$, $n = 3$) and 10 μM thapsigargin ($72 \pm 10\%$, $n = 4$). Each treatment condition differed significantly ($P < 0.03$) from its independent control (Student's two-tailed *t* test).

values significantly different at the 0.05 level (ANOVA) (Fig. 5*D*). Also as in EGTA, the largest initial currents were found with the strongest buffering, but again short of a significant difference. There appeared to be a trend toward less inactivation for equivalent concentrations of BAPTA compared to EGTA (e.g. 28% in 10 mM BAPTA, *versus* 37% in 10 mM EGTA); however, those differences were not statistically significant. As with EGTA buffering, modest residual inactivation remained when barium served as charge carrier, but again this did not vary with buffer concentration.

Inactivation in 2 mM calcium

The foregoing experiments were carried out by eliciting maximal currents (at voltages corresponding to the peak of the *I–V* relation), with 20 mM calcium in the external saline. This calcium concentration was chosen for consistency with earlier work (Martinez-Dunst *et al.* 1997) and to optimize signal-to-noise of the relatively small currents in these cells. The question arises then whether CDI occurs with more physiological calcium loads. Total calcium in chicken serum is $\sim$5 mmol l^{-1} (Prosser & Brown, 1961) while ionized calcium levels range from 1.4 to 1.6 mmol l^{-1}, (e.g. Peltonen *et al.* 2006), and vary significantly during the egg-laying cycle, as well as between males and females. To approximate normal conditions then, calcium-dependent inactivation was also examined with 2 mM external calcium, and compared to 20 mM calcium on a cell-by-cell basis. For seven cells the peak inward current in 2 mM calcium was on average only one-third that in 20 mM calcium (Fig. 6*A*). Nonetheless, the extent and time course of inactivation after a 2 s conditioning voltage step (to the peak of the *I–V* relation)

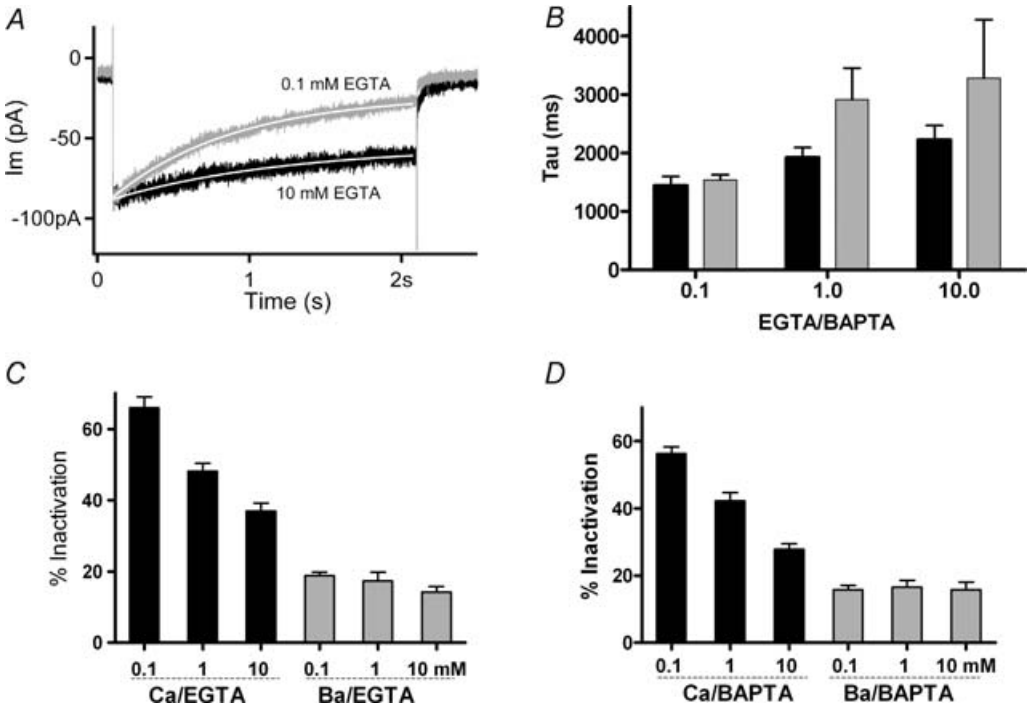

Figure 5. Effects of internal calcium buffering
A, membrane currents in 20 mM external calcium during a 2 s step to 0 mV (from holding voltage −70 mV) from two hair cells with different concentrations of internal EGTA. Peak currents in 0.1 EGTA normalized (by 0.77) to match those in 10 mM EGTA. Single exponentials (continuous white lines) fitted to the current decay yielded time constants of 1.4 s in 0.1 mM EGTA and 2.2 s in 10 mM EGTA. *B*, time constant of inactivation calculated as in *A* for cells in 20 mM external calcium, under different conditions of buffering indicated below each set of two bars (black for EGTA, grey for BAPTA). Time constants in 0.1 mM EGTA and 0.1 mM BAPTA were significantly shorter ($P < 0.03$, ANOVA) than those in the other conditions, which otherwise were not statistically different. *C*, black bars indicate the percentage inactivation of current carried by 20 mM calcium into hair cells buffered with 0.1 mM (66 ± 3.1%, mean ± S.E.M., $n = 14$), 1.0 mM (48 ± 2.2%, $n = 13$) and 10.0 mM (37 ± 2.2%, $n = 12$) EGTA. All means in calcium differ significantly from neighbouring values ($P < 0.03$, ANOVA). Grey bars indicate measurements from the same cells with calcium substituted by 20 mM barium. *D*, black bars indicate percentage inactivation of current carried by 20 mM calcium into hair cells buffered with 0.1 mM (56 ± 1.9%, mean ± S.E.M., $n = 13$), 1.0 mM (42 ± 2.4%, $n = 13$) and 10.0 mM (28 ± 1.6%, $n = 12$) BAPTA. All means in calcium differ significantly from neighbouring values ($P < 0.03$, ANOVA). With barium as charge carrier (grey bars) the percentage inactivation ranged between 14 and 19% with no significant differences between neighbours.

was not significantly different under these two conditions (assessed by voltage ramps). This finding implies that the inactivation process was saturated by prolonged influx from either 20 or 2 mM calcium.

A second question is to what extent CDI occurs at lower levels of calcium channel gating, in particular, near the resting membrane potential at which spontaneous transmitter release occurs. This question was addressed in 2 mM external calcium by alternately holding the membrane potential at −90 or −50 mV for 1 min, then probing calcium channel availability with a voltage ramp. For seven cells the ratio of peak inward currents measured at −50 and −90 mV was 0.50 ± 0.07 (± S.E.M.). The inactivation occurring at −50 mV could be completely reversed by holding again at a negative membrane potential for 1 min (Fig. 6*B*). After correction for leak conductance there was no consistent change in reversal potential or overall position of the *I–V* curve.

Calcium-binding proteins in chicken basilar papilla

Calcium-binding proteins (CaBPs) constitute a family of seven calmodulin-like proteins that are thought to modulate the interactions of calmodulin (CaM) with target binding sites (Haeseleer *et al.* 2002). Nucleotide sequences for mammalian CaBPs were used to scan the chicken genome (NCBI), and three partial coding sequences homologous with mouse and human CaBPs 1, 4 and 7 were identified. Messenger RNA was reverse-transcribed from microdissected lagenar ducts (containing the basilar papilla and lagena). All three orthologous CaBPs could be amplified using specific primers. Nucleotide identities of the RT-PCR products were 77% for CaBP4, 82% for CaBP1, and 89% for CaBP7. The RT-PCR products were translated to the equivalent amino acid sequences and compared to those for mice. Only three conservative amino acid substitutions were predicted by the chicken CaBP1 and CaBP7 cDNAs (Fig. 7*A* and *C*). However, the CaBP4 cDNA from chicken yielded a substantially more variant amino acid sequence, with only ∼70% identical amino acids, although the majority of those changed were for amino acids in the same functional groups (Fig. 7*B*).

Further confirmation of the expression of CaBPs was achieved using antibodies against the mammalian proteins, although these are available only for CaBP1 and CaBP4. When applied to cross-sections from the basilar papilla, antibodies to CaBP1 bound relatively well to the stereociliary bundle and cuticular plate region of hair cells (Fig. 8*A* and *B*) in addition to labelling the tectorial membrane and various cell types in the tegmentum vasculosum. On the other hand, hair cell cytoplasm, and in particular, the synaptic pole of tall (inner-like) hair cells, were not well labelled. Although cholinergic efferent neurons preferentially label short, outer-like hair cells in chicken (Zidanic & Fuchs, 1996; Zidanic, 2002), a few efferent endings labelled red with antibodies against choline acetyl-transferase (ChAT) demarcate the synaptic pole of tall hair cells in Fig. 8. When antibodies to CaBP4 were employed, tectorial membrane and tegmentum vasculosum were essentially unlabelled, but more robust labelling of hair cell somata was achieved (Fig. 8*B*). Stereociliary bundles, however, were not labelled. In contrast to the pattern seen with antibodies to CaBP1, CaBP4 antibodies labelled the synaptic pole of the hair cells

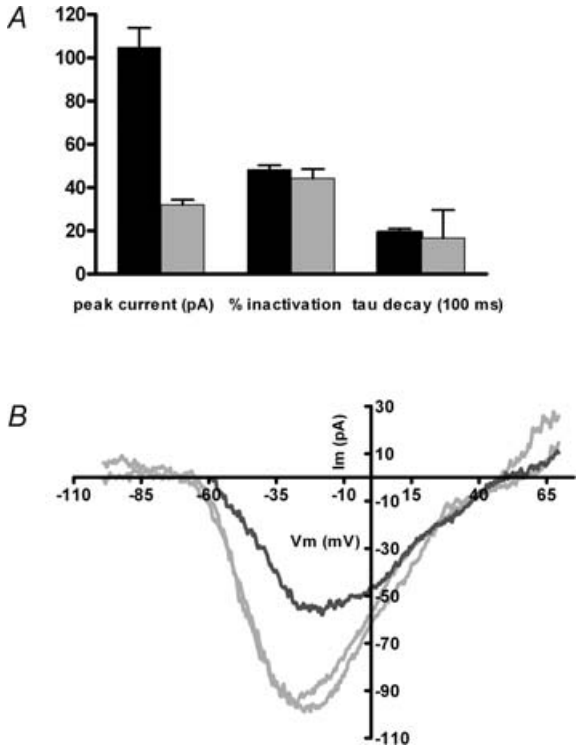

Figure 6. Inactivation in 'physiological' external calcium
A, inward currents were measured in 13 cells exposed successively to 2 and 20 mM external calcium (1.0 mM EGTA internal buffer). Peak inward currents and percentage inactivation were determined from voltage ramps executed before and after a 2 s depolarization to the peak of the *I–V* relation from −70 mV holding voltage. The time constant of inactivation was taken from a single exponential fit to the current during the inactivating step. Only peak currents were significantly different (105 ± 8.8 pA, mean ± S.E.M., $n = 13$ in 20 mM calcium; 32 ± 2.4 pA, in 2 mM calcium, $n = 13$). The percentage inactivation in 20 mM calcium (48 ± 2.1%, mean ± S.E.M.) and in 2 mM calcium (44 ± 4.3%) was not different (nor did it differ from the independent measurements averaged in Fig. 5, 48 ± 2.2%), nor was the time constant of decay significantly different (1.9 ± 0.2 and 1.7 ± 0.3 s, mean ± S.E.M., in 20 and 2 mM calcium, respectively). *B*, voltage ramps evoked inward currents in 2 mM external calcium from a holding potential of −90 mV (grey traces) before and after an *I–V* collected at −50 mV holding potential (black trace). In 7 such experiments, the ratio of peak inward currents obtained at −50 mV to those from −90 mV was 0.50 ± 0.20 (mean ± S.E.M.). The average recovery value (comparing the *I–V* peak from −90 mV before and 1 min after inactivation) was 0.82 ± 0.08.

as strongly as the cuticular plates. These same patterns of labelling were achieved in four separate preparations.

Discussion

The present work was designed to establish the extent of calcium-dependent inactivation of hair cells in the chicken basilar papilla (analogous to the mammalian cochlea). This model was chosen as a representative vertebrate whose auditory epithelium shares features of structure and function with those of both cold-blooded reptiles and mammals (Fuchs *et al.* 1988; Fischer, 1992; Fuchs & Murrow, 1992), and for which substantial auditory nerve data also exist (e.g. Saunders *et al.* 2002). Prolonged (2 s) maximal calcium currents produced significant inactivation that was itself calcium dependent. The extent of inactivation in any one hair cell depended on the magnitude of calcium influx (i.e. as adjusted by changing membrane potential and so driving force on influx). Higher concentrations of internal calcium buffer (10 mM) reduced the extent of inactivation, while lower levels of buffer (0.1 mM) were associated with more rapid, more extensive inactivation.

Several observations suggest that CDI depended on the relatively gradual accumulation of calcium into an as-yet undefined 'activation volume'. First, the time constant of CDI was slow, nearly 2 s for maximal currents with 1 mM EGTA internal buffering, with a recovery half-time of 10 s. Secondly, the extent of inactivation was not significantly different whether EGTA or BAPTA was used as the internal calcium buffer, arguing that the more rapid binding kinetic of BAPTA was irrelevant to this gradual process. Finally, reduced activity of endoplasmic calcium pumps increased the extent and hastened the time course of CDI, as though

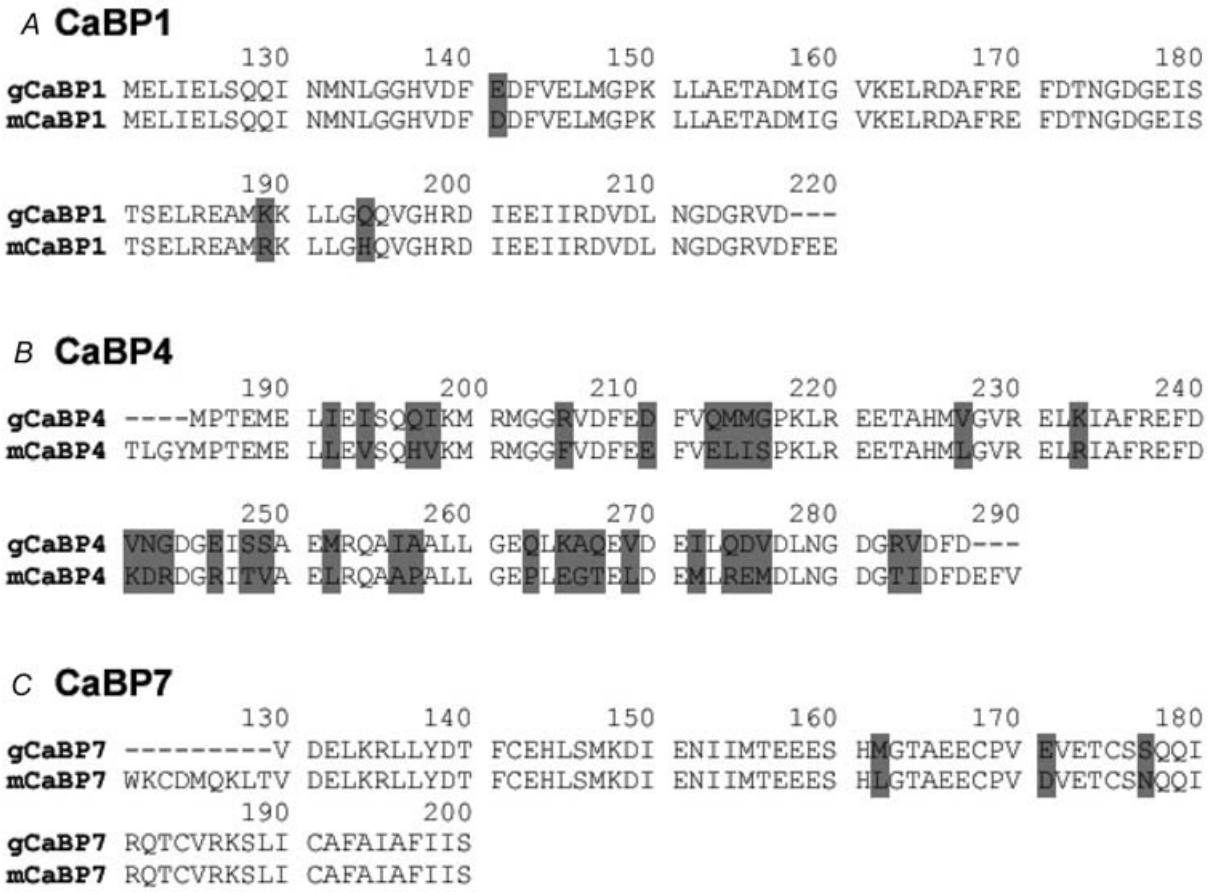

Figure 7. CaBPs in chicken basilar papilla
RT-PCR using specific chicken CaBP sequences (derived by homology search of the chicken genome with mouse CaBPs) amplified products corresponding to mammalian orthologues of CaBPs 1, 4 and 7. The derived sequences were translated to amino acids and compared to their mouse orthologues, with variant amino acids indicated by grey background. *A*, an RT-PCR product corresponding to 97 amino acids of mouse CaBP1 differed by only 3 conserved substitutions. *B*, the CaBP4 RT-PCR product encoded 103 amino acids, of which 72 were identical and 20 were conserved substitutions compared to the mouse CaBP4 sequence, the remainder being changes to dissimilar amino acids. *C*, the RT-PCR product encoding 71 amino acids corresponding to mouse CaBP7 had only 3 conservative amino acid substitutions.

a causal cytoplasmic calcium pool was enhanced. One possible interpretation of these observations is that CDI involves a process such as a phosphorylation cascade in which calcium-dependent kinases are involved. Activity in this cascade would vary in proportion to free calcium in the cytoplasm, itself a product of influx, buffering and pumping.

Given this hypothesis, it is of interest that the extent of inactivation did not vary with peak calcium current among the population of cells studied. The implication is that the cell-to-cell variation in calcium channel number (peak current) is accompanied by equivalent variation in associated mechanisms of calcium homeostasis. This is consistent with the supposition that calcium channels are clustered specifically at ribbon synapses in chicken (Martinez-Dunst *et al.* 1997) as in other species (Roberts *et al.* 1990; Issa & Hudspeth, 1994; Ricci *et al.* 2000; Khimich *et al.* 2005). That is, each cluster of calcium channels generates its own local calcium load, regulated by local calcium stores and other homeostatic mechanisms. Variations in the extent of inactivation between cells could result from the relative positioning of ribbons (density), such that local calcium loads could overlap, or that fixed buffer efficacy (endoplasmic stores) varied between cells. The other related observation is that CDI was equivalent whether external calcium was 2 or 20 mM. Apparently then, the cytoplasmic 'activation volume' for calcium was saturated by prolonged influx from either of these conditions. This is not entirely surprising since the total change in driving force was theoretically less than 20% (26 mV out of ~150 mV). However, this supposition will depend on total buffer concentration. Finally, CDI was substantial even for moderate levels of calcium influx. The peak calcium current was reduced by 50% when hair cells were simply held at −50 mV, near the presumptive *in vivo* membrane potential and near the foot of the calcium activation curve.

Studies of auditory hair cells of reptiles (Schnee & Ricci, 2003) and mice (Marcotti *et al.* 2003; Michna *et al.* 2003) also have shown that voltage-gated calcium currents inactivate. In turtle hair cells, for example, inactivation was sensitive to substitution of calcium with barium, and the extent of inactivation fell approximately 30% when internal BAPTA was raised from 1 to 30 mM. A virtually identical degree of inactivation of calcium currents (~50%) was obtained in turtle and chicken hair cells by a 40 mV change in holding potential. In contrast, inactivation in turtle hair cells was relatively insensitive to calcium buffering when compared to that in chicken, and barium preserved inactivation to a larger extent in turtle than in chicken hair cells. It is not known yet whether the L-type calcium channels of turtle possess calmodulin-binding sites, so the molecular basis for these distinctions remains to be explored. Inactivation has been reported in both inner (Marcotti *et al.* 2003) and outer (Michna *et al.* 2003) hair cells of the neonatal mammalian cochlea. In both cell types inactivation was dependent on external calcium and the calcium driving force as expected for CDI. It was not determined whether CDI varied with internal calcium buffering or alterations in calcium store function.

CDI has been described at other 'tonic' (ribbon-dependent) synapses. In bipolar cell terminals from goldfish retina (von Gersdorff & Matthews, 1996) the extent and time course of CDI were strikingly similar to that reported here in chicken hair cells and, as in the present report, lower concentrations of internal calcium buffer were associated with more extensive CDI. The similarities between these two systems may not be accidental. Both goldfish bipolar cells (Logiudice *et al.* 2006) and chicken cochlear hair cells (Kollmar *et al.* 1997*b*) express $Ca_V1.3$ (α1D), a member of the

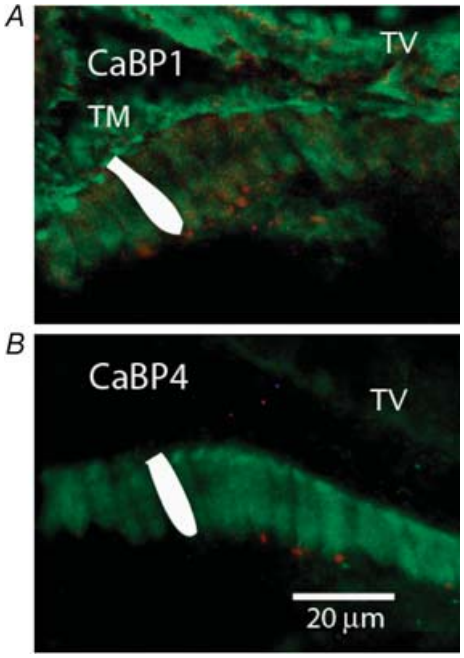

Figure 8. CaBP antibody labelling in chicken basilar papilla
Antibodies available for CaBP1 and CaBP4 were used to label cryosections (across the long axis) of the chicken basilar papilla. Tegmentum vasculosum (collapsed onto basilar papilla) is labelled 'TV'. Tectorial membrane (visible only in *A*) is labelled 'TM'. A single hair cell is shaded white in each image for reference. *A*, antiserum to CaBP1 (green) bound to hair cells and supporting cells in the basilar papilla, to the tectorial membrane, and to cells in the tegmentum vasculosum. Immunolabelling of hair cells was concentrated in the cuticular plate and hair bundle. Antibody to choline acetyl-transferase (ChAT, red) indicates the position of efferent cholinergic endings located on the synaptic pole of hair cells. *B*, antiserum to CaBP4 (green) strongly labelled hair cells in the basilar papilla, and TV very faintly. Hair cell cytoplasm labelled as strongly as cuticular plate (hair bundles did not label). Each image has been optimized for brightness and contrast, so relative intensities cannot be compared between panels. ChAT antibody label (in red) indicates efferent boutons at synaptic pole of hair cells.

dihydropyridine-sensitive L-type family of voltage-gated calcium channels. This also is the predominant gene encoding voltage-gated calcium channels in mammalian cochlear hair cells (Platzer *et al.* 2000). Recent studies have raised the possibility that CDI of these channels can be modulated by calmodulin-like calcium-binding proteins (CaBPs) (Yang *et al.* 2006). These proteins may alter the action of calmodulin bound to IQ domains on the carboxy tail of $Ca_V1.3$, thereby disrupting CDI that depends on calmodulin. CaBPs were first identified in mammalian retina (Haeseleer *et al.* 2000). CaBP4 was found to be expressed specifically in photoreceptor terminals (Haeseleer *et al.* 2004) and subsequently in inner hair cells of the rat cochlea (Yang *et al.* 2006). However, unlike hair cells the photoreceptors express a different L-type calcium channel, $Ca_V1.4$, that does not inactivate when expressed in heterologous cells (McRory *et al.* 2004). Thus, coexpression with CaBP4 had no impact on inactivation, but did cause a negative shift in the voltage activation range of $Ca_V1.4$ (Haeseleer *et al.* 2004). Functional interactions are likely, then, to depend on both the specific channel type, including splice variants (Kollmar *et al.* 1997*a*; Ramakrishnan *et al.* 2002; Shen *et al.* 2006), and which of the family of calmodulin-like proteins are present in each cell type. In this context it is interesting that the partial sequence for CaBP4 found here was more variant from mouse than that for either CaBP1 or CaBP7. One might speculate that greater functional specialization has occurred for this 'synaptic' calcium-binding protein.

What functional role might CDI play in chicken cochlear hair cells? The slow time course argues against participation in adaptation of afferent nerve firing that occurs within ~20 ms (Crumling & Saunders, 2007), and has a temperature Q_{10} of only 1.2 (Crumling & Saunders, 2005). Afferent nerve adaptation in chicken may reflect exhaustion of presynaptic vesicular pools (Spassova *et al.* 2004). Rather, CDI as observed in the present work could be important as a negative feedback mechanism that adjusts the 'steady-state' number of available calcium channels. This becomes particularly critical considering the limited number of calcium channels available to each ribbon. The relation between ribbon size and calcium current amplitude (Martinez-Dunst *et al.* 1997) implies that hair cells largely restrict channel expression to release sites, thereby minimizing total calcium flux. Indeed various studies report that only a small number of channels, 100 or fewer, will be found at each synaptic ribbon (Roberts *et al.* 1990; Martinez-Dunst *et al.* 1997; Brandt *et al.* 2005; Fuchs, 2005) and modelling studies suggest that small, dense channel clusters will provide the best temporal resolution for synaptic release (Wu *et al.* 1996). With such a limited pool of channels to draw upon, the hair cell must ensure that some level of release continues even at rest, while simultaneously preserving the widest possible dynamic range. A negative feedback process such as steady-state CDI observed in the present work is able to make such adjustments, providing that CDI itself can be fine-tuned to each cell's specific needs. We propose that calmodulin-like calcium-binding proteins could serve this role in avian, as in mammalian hair cells.

References

Art JJ & Fettiplace R (1987). Variation of membrane properties in hair cells isolated from the turtle cochlea. *J Physiol* **385**, 207–242.

Art JJ, Fettiplace R & Wu YC (1993). The effects of low calcium on the voltage-dependent conductances involved in tuning of turtle hair cells. *J Physiol* **470**, 109–126.

Bao H, Wong WH, Goldberg JM & Eatock RA (2003). Voltage-gated calcium channel currents in type I and type II hair cells isolated from the rat crista. *J Neurophysiol* **90**, 155–164.

Beutner D & Moser T (2001). The presynaptic function of mouse cochlear inner hair cells during development of hearing. *J Neurosci* **21**, 4593–4599.

Brandt A, Khimich D & Moser T (2005). Few $Ca_V1.3$ channels regulate the exocytosis of a synaptic vesicle at the hair cell ribbon synapse. *J Neurosci* **25**, 11577–11585.

Brandt A, Striessnig J & Moser T (2003). $Ca_V1.3$ channels are essential for development and presynaptic activity of cochlear inner hair cells. *J Neurosci* **23**, 10832–10840.

Chen L, Salvi R & Shero M (1994). Cochlear frequency-place map in adult chickens: intracellular biocytin labeling. *Hear Res* **81**, 130–136.

Crawford AC & Fettiplace R (1981). An electrical tuning mechanism in turtle cochlear hair cells. *J Physiol* **312**, 377–412.

Crumling MA & Saunders JC (2005). Temperature insensitivity of short-term adaptation in single-units of the chick cochlear nerve. *Synapse* **58**, 243–248.

Crumling MA & Saunders JC (2007). Tonotopic distribution of short-term adaptation properties in the cochlear nerve of normal and acoustically overexposed chicks. *J Assoc Res Otolaryngol* **8**, 54–68.

Dou H, Vazquez AE, Namkung Y, Chu H, Cardell EL, Nie L, Parson S, Shin HS & Yamoah EN (2004). Null mutation of α_{1D} Ca^{2+} channel gene results in deafness but no vestibular defect in mice. *J Assoc Res Otolaryngol* **5**, 215–226.

Engel J, Michna M, Platzer J & Striessnig J (2002). Calcium channels in mouse hair cells: function, properties and pharmacology. *Adv Otorhinolaryngol* **59**, 35–41.

Fischer FP (1992). Quantitative analysis of the innervation of the chicken basilar papilla. *Hear Res* **61**, 167–178.

Fuchs PA (2005). Time and intensity coding at the hair cell's ribbon synapse. *J Physiol* **566**, 7–12.

Fuchs PA & Evans MG (1990). Potassium currents in hair cells isolated from the cochlea of the chick. *J Physiol* **429**, 529–551.

Fuchs PA, Evans MG & Murrow BW (1990). Calcium currents in hair cells isolated from the cochlea of the chick. *J Physiol* **429**, 553–568.

Fuchs PA & Murrow BW (1992). Cholinergic inhibition of short (outer) hair cells of the chick's cochlea. *J Neurosci* **12**, 800–809.

Fuchs PA, Nagai T & Evans MG (1988). Electrical tuning in hair cells isolated from the chick cochlea. *J Neurosci* **8**, 2460–2467.

Fuchs PA & Sokolowski BH (1990). The acquisition during development of Ca-activated potassium currents by cochlear hair cells of the chick. *Proc R Soc Lond B Biol Sci* **241**, 122–126.

Green GE, Khan KM, Beisel DW, Drescher MJ, Hatfield JS & Drescher DG (1996). Calcium channel subunits in the mouse cochlea. *J Neurochem* **67**, 37–45.

Haeseleer F, Imanishi Y, Maeda T, Possin DE, Maeda A, Lee A, Rieke F & Palczewski K (2004). Essential role of Ca^{2+}-binding protein 4, a $Ca_v1.4$ channel regulator, in photoreceptor synaptic function. *Nat Neurosci* **7**, 1079–1087.

Haeseleer F, Imanishi Y, Sokal I, Filipek S & Palczewski K (2002). Calcium-binding proteins: intracellular sensors from the calmodulin superfamily. *Biochem Biophys Res Commun* **290**, 615–623.

Haeseleer F, Sokal I, Verlinde CL, Erdjument-Bromage H, Tempst P, Pronin AN, Benovic JL, Fariss RN & Palczewski K (2000). Five members of a novel Ca^{2+}-binding protein (CABP) subfamily with similarity to calmodulin. *J Biol Chem* **275**, 1247–1260.

Hafidi A & Dulon D (2004). Developmental expression of $Ca_v1.3$ (α1d) calcium channels in the mouse inner ear. *Brain Res Dev Brain Res* **150**, 167–175.

Hiel H, Navaratnam DS, Oberholtzer JC & Fuchs PA (2002). Topological and developmental gradients of calbindin expression in the chick's inner ear. *J Assoc Res Otolaryngol* **3**, 1–15.

Issa NP & Hudspeth AJ (1994). Clustering of Ca^{2+} channels and Ca^{2+}-activated K^+ channels at fluorescently labeled presynaptic active zones of hair cells. *Proc Natl Acad Sci U S A* **91**, 7578–7582.

Khimich D, Nouvian R, Pujol R, Tom Dieck S, Egner A, Gundelfinger ED & Moser T (2005). Hair cell synaptic ribbons are essential for synchronous auditory signaling. *Nature* **434**, 889–894.

Kollmar R, Fak J, Montgomery LG & Hudspeth AJ (1997*a*). Hair cell-specific splicing of mRNA for the α_{1D} subunit of voltage-gated Ca^{2+} channels in the chicken's cochlea. *Proc Natl Acad Sci U S A* **94**, 14889–14893.

Kollmar R, Montgomery LG, Fak J, Henry LJ & Hudspeth AJ (1997*b*). Predominance of the α_{1D} subunit in L-type voltage-gated Ca^{2+} channels of hair cells in the chicken's cochlea. *Proc Natl Acad Sci U S A* **94**, 14883–14888.

Kros CJ, Ruppersberg JP & Rüsch A (1998). Expression of a potassium conductance in inner hair cells at the onset of hearing in mice. *Nature* **394**, 281–284.

Lewis RS & Hudspeth AJ (1983). Voltage- and ion-dependent conductances in solitary vertebrate hair cells. *Nature* **304**, 538–541.

Liang H, DeMaria CD, Erickson MG, Mori MX, Alseikhan BA & Yue DT (2003). Unified mechanisms of Ca^{2+} regulation across the Ca^{2+} channel family. *Neuron* **39**, 951–960.

Logiudice L, Henry D & Matthews G (2006). Identification of calcium channel α1 subunit mRNA expressed in retinal bipolar neurons. *Mol Vis* **12**, 184–189.

McRory JE, Hamid J, Doering CJ, Garcia E, Parker R, Hamming K, Chen L, Hildebrand M, Beedle AM, Feldcamp L, Zamponi GW & Snutch TP (2004). The *CACNA1F* gene encodes an L-type calcium channel with unique biophysical properties and tissue distribution. *J Neurosci* **24**, 1707–1718.

Marcotti W, Johnson SL & Kros CJ (2004). A transiently expressed SK current sustains and modulates action potential activity in immature mouse inner hair cells. *J Physiol* **560**, 691–708.

Marcotti W, Johnson SL, Rusch A & Kros CJ (2003). Sodium and calcium currents shape action potentials in immature mouse inner hair cells. *J Physiol* **552**, 743–761.

Martinez-Dunst C, Michaels RL & Fuchs PA (1997). Release sites and calcium channels in hair cells of the chick's cochlea. *J Neurosci* **17**, 9133–9144.

Martini M, Rispoli G, Farinelli F, Fesce R & Rossi ML (2004). Intracellular Ca^{2+} buffers can dramatically affect Ca^{2+} conductances in hair cells. *Hear Res* **195**, 67–74.

Matthews TM, Duncan RK, Zidanic M, Michael TH & Fuchs PA (2005). Cloning and characterization of SK2 channel from chicken short hair cells. *J Comp Physiol Neuroethol Sens Neural Behav Physiol* **191**, 491–503.

Merchan-Perez A & Liberman MC (1996). Ultrastructural differences among afferent synapses on cochlear hair cells: correlations with spontaneous discharge rate. *J Comp Neurol* **371**, 208–221.

Michna M, Knirsch M, Hoda JC, Muenkner S, Langer P, Platzer J, Striessnig J & Engel J (2003). $Ca_v1.3$ (α1D) Ca^{2+} currents in neonatal outer hair cells of mice. *J Physiol* **553**, 747–758.

Murrow BW (1994). Position-dependent expression of potassium currents by chick cochlear hair cells. *J Physiol* **480**, 247–259.

Nakagawa T, Kakehata S, Akaike N, Komune S, Takasaka T & Uemura T (1991). Calcium channel in isolated outer hair cells of guinea pig cochlea. *Neurosci Lett* **125**, 81–84.

Peltonen LM, Sankari S, Kivimaki A & Autio P (2006). Novel function of the skin in calcium metabolism in female and male chickens (*Gallus domesticus*). *Comp Biochem Physiol B Biochem Mol Biol* **144**, 432–441.

Platzer J, Engel J, Schrott-Fischer A, Stephan K, Bova S, Chen H, Zheng H & Striessnig J (2000). Congenital deafness and sinoatrial node dysfunction in mice lacking class D L-type Ca^{2+} channels. *Cell* **102**, 89–97.

Prigioni I, Masetto S, Russo G & Taglietti V (1992). Calcium currents in solitary hair cells isolated from frog crista ampullaris. *J Vestib Res* **2**, 31–39.

Prosser CL & Brown FA (1961). *Comparative Animal Physiology*. W. B. Saunders Company, Philadelphia.

Ramakrishnan NA, Green GE, Pasha R, Drescher MJ, Swanson GS, Perin PC, Lakhani RS, Ahsan SF, Hatfield JS, Khan KM & Drescher DG (2002). Voltage-gated Ca^{2+} channel $Ca_V1.3$ subunit expressed in the hair cell epithelium of the sacculus of the trout *Oncorhynchus mykiss*: cloning and comparison across vertebrate classes. *Brain Res Mol Brain Res* **109**, 69–83.

Ricci AJ, Gray-Keller M & Fettiplace R (2000). Tonotopic variations of calcium signalling in turtle auditory hair cells. *J Physiol* **524**, 423–436.

Rispoli G, Martini M, Rossi ML, Rubbini G & Fesce R (2000). Ca^{2+}-dependent kinetics of hair cell Ca^{2+} currents resolved with the use of cesium BAPTA. *Neuroreport* **11**, 2769–2774.

Roberts WM, Jacobs RA & Hudspeth AJ (1990). Colocalization of ion channels involved in frequency selectivity and synaptic transmission at presynaptic active zones of hair cells. *J Neurosci* **10**, 3664–3684.

Robertson D & Paki B (2002). Role of L-type Ca^{2+} channels in transmitter release from mammalian inner hair cells. II. Single-neuron activity. *J Neurophysiol* **87**, 2734–2740.

Rodriguez-Contreras A & Yamoah EN (2001). Direct measurement of single-channel Ca^{2+} currents in bullfrog hair cells reveals two distinct channel subtypes. *J Physiol* **534**, 669–689.

Salvi RJ, Saunders SS, Powers NL & Boettcher FA (1992). Discharge patterns of cochlear ganglion neurons in the chicken. *J Comp Physiol [A]* **170**, 227–241.

Saunders JC, Ventetuolo CE, Plontke SK & Weiss BA (2002). Coding of sound intensity in the chick cochlear nerve. *J Neurophysiol* **88**, 2887–2898.

Schnee ME & Ricci AJ (2003). Biophysical and pharmacological characterization of voltage-gated calcium currents in turtle auditory hair cells. *J Physiol* **549**, 697–717.

Shen Y, Yu D, Hiel H, Liao P, Yue DT, Fuchs PA & Soong TW (2006). Alternative splicing of the $Ca_v1.3$ channel IQ domain, a molecular switch for Ca^{2+}-dependent inactivation within auditory hair cells. *J Neurosci* **26**, 10690–10699.

Sokolowski BH, Stahl LM & Fuchs PA (1993). Morphological and physiological development of vestibular hair cells in the organ-cultured otocyst of the chick. *Dev Biol* **155**, 134–146.

Spassova MA, Avissar M, Furman AC, Crumling MA, Saunders JC & Parsons TD (2004). Evidence that rapid vesicle replenishment of the synaptic ribbon mediates recovery from short-term adaptation at the hair cell afferent synapse. *J Assoc Res Otolaryngol* **5**, 376–390.

Su ZL, Jiang SC, Gu R & Yang WP (1995). Two types of calcium channels in bullfrog saccular hair cells. *Hear Res* **87**, 62–68.

Tucker TR & Fettiplace R (1996). Monitoring calcium in turtle hair cells with a calcium-activated potassium channel. *J Physiol* **494**, 613–626.

von Gersdorff H & Matthews G (1996). Calcium-dependent inactivation of calcium current in synaptic terminals of retinal bipolar neurons. *J Neurosci* **16**, 115–122.

Wu YC, Tucker T & Fettiplace R (1996). A theoretical study of calcium microdomains in turtle hair cells. *Biophys J* **71**, 2256–2275.

Yang PS, Alseikhan BA, Hiel H, Grant L, Mori MX, Yang W, Fuchs PA & Yue DT (2006). Switching of Ca^{2+}-dependent inactivation of $Ca_v1.3$ channels by calcium binding proteins of auditory hair cells. *J Neurosci* **26**, 10677–10689.

Yuhas WA & Fuchs PA (1999). Apamin-sensitive, small-conductance, calcium-activated potassium channels mediate cholinergic inhibition of chick auditory hair cells. *J Comp Physiol [A]* **185**, 455–462.

Zidanic M (2002). Cholinergic innervation of the chick basilar papilla. *J Comp Neurol* **445**, 159–175.

Zidanic M & Fuchs PA (1995). Kinetic analysis of barium currents in chick cochlear hair cells. *Biophys J* **68**, 1323–1336.

Zidanic M & Fuchs PA (1996). Efferent synaptic endings in the chick's cochlea revealed by synapsin immunohistochemistry. *Aud Neurosci* **2**, 347–362.

Acknowledgements

This work was supported by grants R01 DC000276 and P30 DC005211 from the National Institute for Deafness and Communication Disorders to P.F. and a research fellowship to S.L. from the Department of Otolaryngology – Head and Neck Surgery, Hanyang University, Seoul, Korea. We thank Francoise Haeseleer for CaBP antibodies.